

Net carbon dioxide losses of northern ecosystems in response to autumn warming

Shilong Piao¹, Philippe Ciais¹, Pierre Friedlingstein¹, Philippe Peylin², Markus Reichstein³, Sebastiaan Luyssaert⁴, Hank Margolis⁵, Jingyun Fang⁶, Alan Barr⁷, Anping Chen⁸, Achim Grelle⁹, David Y. Hollinger¹⁰, Tuomas Laurila¹¹, Anders Lindroth¹², Andrew D. Richardson¹³ & Timo Vesala¹⁴

The carbon balance of terrestrial ecosystems is particularly sensitive to climatic changes in autumn and spring^{1–4}, with spring and autumn temperatures over northern latitudes having risen by about 1.1 °C and 0.8 °C, respectively, over the past two decades⁵. A simultaneous greening trend has also been observed, characterized by a longer growing season and greater photosynthetic activity^{6,7}. These observations have led to speculation that spring and autumn warming could enhance carbon sequestration and extend the period of net carbon uptake in the future⁸. Here we analyse interannual variations in atmospheric carbon dioxide concentration data and ecosystem carbon dioxide fluxes. We find that atmospheric records from the past 20 years show a trend towards an earlier autumn-to-winter carbon dioxide build-up, suggesting a shorter net carbon uptake period. **This trend cannot be explained by changes in atmospheric transport alone and, together with the ecosystem flux data, suggest increasing carbon losses in autumn.** We use a process-based terrestrial biosphere model and satellite vegetation greenness index observations to investigate further the observed seasonal response of northern ecosystems to autumnal warming. **We find that both photosynthesis and respiration increase during autumn warming, but the increase in respiration is greater.** In contrast, warming increases photosynthesis more than respiration in spring. **Our simulations and observations indicate that northern terrestrial ecosystems may currently lose carbon dioxide in response to autumn warming, with a sensitivity of about 0.2 PgC °C⁻¹, offsetting 90% of the increased carbon dioxide uptake during spring.** If future autumn warming occurs at a faster rate than in spring, the ability of northern ecosystems to sequester carbon may be diminished earlier than previously suggested^{9,10}.

The carbon balance of terrestrial ecosystems is highly sensitive to climate changes at the edges of the growing season^{1–4}. In response to warmer springs, for example, several field studies have shown that boreal forests absorb more carbon^{11,12} as a result of an earlier beginning of the growing season^{13,14}. A strong autumn warming is currently occurring in eastern Asia and eastern North America¹⁵. However, little attention has been given to the impacts of this forcing on the terrestrial carbon cycle. We have analysed how interannual variations and trends in autumn temperatures have recently affected atmospheric CO₂ concentrations, ecosystem CO₂ fluxes measured by eddy covariance, and remotely sensed vegetation greenness values. A

process-oriented terrestrial biosphere model (ORCHIDEE)¹⁶ is combined with an atmospheric transport model (LMDZt)¹⁷ to quantify the processes through which autumn warming controls the carbon balance of ecosystems (see Methods).

The seasonal cycle of atmospheric CO₂ concentrations provides an integrated measure of the net land–atmosphere carbon exchange (net ecosystem productivity; NEP) and its temporal characteristics^{18,19}. We analysed the ten atmospheric CO₂ measurement records from the NOAA–ESRL air-sampling network²⁰, which cover at least 15 years of data in the Northern Hemisphere (Fig. 1 and Supplementary Table 1). The upward zero-crossing date of CO₂ was determined as the day when the de-trended atmospheric CO₂ seasonal cycle crosses the zero line from negative to positive values (see Methods). This date occurs in autumn at northern high-latitude stations and in early winter at northern tropical stations (Supplementary Table 1). We found that variations in the CO₂ zero-crossing date are negatively correlated with anomalies in autumn air temperatures⁵ over a broad region surrounding each station by ±20° of latitude. All CO₂ records show a negative correlation, with four out of ten sites having statistically significant correlations (Supplementary Table 2). The probability that this occurs purely by chance is estimated to be about 10⁻⁵ if all station records are assumed to be independent (see Supplementary Information). The striking anti-correlation between autumnal temperature and CO₂ zero-crossing date is illustrated in Fig. 1a for the 23-year-long atmospheric measurement record of Point Barrow in northern Alaska ($R = -0.61$, $P = 0.002$). In contrast with the widespread influence of temperature, the upward CO₂ zero-crossing date shows no significant correlation with precipitation anomalies (Supplementary Table 2). If soil moisture calculated by the ORCHIDEE model (see Methods) is used instead of precipitation as a predictor of CO₂ upward zero-crossing dates, then only six of the ten sites show a positive correlation, and only three of the ten sites show a higher correlation with soil moisture than with temperature. Similar results are also inferred from a partial correlation analysis in which the controlling effects of other variables on temperature were removed (Supplementary Table 2).

We verified that the strong negative correlation between upward CO₂ zero-crossing date and temperature predominantly reflects climate-driven fluctuations in NEP, rather than interannual fluctuations in atmospheric transport. To do so, we prescribed either variable NEP or climatological NEP fluxes from ORCHIDEE to the

¹LSCE, UMR CEA-CNRS, Bâtiment 709, CE, L'Orme des Merisiers, F-91191 Gif-sur-Yvette, France. ²Laboratoire de Biogéochimie Isotopique, LBI, Bâtiment EGER, F-78026 Thiverval-Grignon, France. ³Max Planck Institute for Biogeochemistry, PO Box 100164, 07701 Jena, Germany. ⁴Department of Biology, University of Antwerp, Universiteitsplein 1, 2610 Wilrijk, Belgium. ⁵Faculté de foresterie et de géomatique, Université Laval, Sainte-Foy, Québec G1K 7P4, Canada. ⁶Department of Ecology, Peking University, Beijing 100871, China. ⁷Climate Research Division, Environment Canada, 11 Innovation Boulevard, Saskatoon, Saskatchewan S7N 3H5, Canada. ⁸Department of Ecology and Evolutionary Biology, Princeton University, Princeton, New Jersey 08544, USA. ⁹Department of Ecology, Swedish University of Agricultural Sciences, SE-750 07 Uppsala, Sweden. ¹⁰USDA Forest Service Northern Research Station, 271 Mast Road, Durham, New Hampshire 03824, USA. ¹¹Finnish Meteorological Institute, FIN-00101 Helsinki, Finland. ¹²Department of Physical Geography and Ecosystems Analysis, Lund University, SE-22362 Lund, Sweden. ¹³Complex Systems Research Center, University of New Hampshire, Durham, New Hampshire 03824, USA. ¹⁴Department of Physical Sciences, University of Helsinki, PO Box 64, FIN-00014 Helsinki, Finland.

global transport model LMDZt driven by variable wind fields (see Methods). With the exception of the Mt Cimone (CMN) and Cape Kumukahi (KUM) stations, we found that the fluctuations in upward zero-crossing dates are driven mainly by changes in NEP, and only partly by interannual wind changes (see Methods, Supplementary Table 3 and Supplementary Fig. 1). We also verified that accounting for increasing ocean uptake and fossil fuel emissions in the LMDZt transport model did not significantly affect the zero-crossing dates because these two fluxes contribute less than 4% of the variation for all sites (except for station KUM). The possible changes in seasonal fossil fuel emissions over time may only marginally impact the upward CO₂ zero-crossing date changes (see Methods).

There is also a long-term trend in the autumn upward zero-crossing date of atmospheric CO₂ superimposed on interannual fluctuations. At Point Barrow, for instance, we determined a systematic advance of $-0.40 \text{ day yr}^{-1}$ (Fig. 1b), which was not primarily caused by changes in atmospheric transport, because the trends in zero-crossing date simulated with climatological ORCHIDEE fluxes and interannual transport are only about $-0.12 \text{ day yr}^{-1}$. Overall, eight of ten sites show an earlier trend in upward zero-crossing date, with four sites being statistically significant (Fig. 1b). This trend towards earlier or increased ecosystem losses of CO₂ in autumn becomes

apparent when analysing CO₂ data from the past decade, whereas it was non-existent in the CO₂ data from 1970 to 1994 (ref. 18) as a result of the time-frame of their analysis. This trend towards larger autumn CO₂ losses is not a legacy from drier summers²¹, because atmospheric CO₂ data show that weaker summer CO₂ minima are not significantly associated with an advanced upward zero-crossing date at all sites. The advance in autumnal atmospheric CO₂ zero-crossing date clearly exceeds that of the spring zero-crossing date (Supplementary Table 3). Thus, the duration of the net carbon uptake period (CUP), defined as the difference between autumn upward and spring downward CO₂ zero-crossing dates, has on average decreased at nearly all Northern Hemisphere atmospheric CO₂ stations (Fig. 1b).

Next, we analysed 108 site-years of eddy-covariance CO₂ measurement data from 24 northern ecosystem sites (Supplementary Table 4) to quantify the response of the CUP ending date to interannual variations in autumn temperature (see Methods). All sites combined show that the CUP terminates systematically earlier when autumn conditions are warmer, and vice versa (Fig. 2). Further, stronger temperature anomalies seem to have stronger effects on ecosystem carbon balance than weak anomalies ($P < 0.05$). Hence, despite a large scatter in the individual yearly eddy-covariance CUP dates (see insets to Fig. 2), these micrometeorological observations corroborate the atmospheric concentration records.

The large-scale atmospheric concentration records, taken together with the ecosystem-scale eddy-covariance flux measurements (about 1 km^2) suggest that warmer temperatures in autumn increase ecosystem CO₂ losses by shortening the net CUP. This finding stands in apparent contradiction of the autumn 'greening' and longer-lasting vegetation activity detected at mid-to-high northern latitudes by remote sensing^{6,7} and by numerous *in situ* phenological indicators^{13,22}. However, the underlying mechanisms and processes are yet to be explained. NEP results from the balance between gross primary photosynthesis (GPP) and total ecosystem respiration (TER), necessitating separate investigations into the response of each gross flux to temperature changes. We provide some indication of possible controlling mechanisms by using the ORCHIDEE terrestrial biosphere simulation model forced by variable climate fields over the period 1980–2002 (see Methods). The model's ability to capture the timing of the CUP and the length of the growing season successfully was verified by using the following: first, eddy-covariance CO₂ flux measurements^{16,23}, second, satellite-derived observations of global leaf area index²⁴, and third, interannual and seasonal variations in atmospheric CO₂ (see Methods and Supplementary Fig. 1). Results from these studies suggest that it is possible to use this model tool to help in disentangling the response of photosynthesis, respiration and NEP to climate variability.

Simulated September to November NEP shows a trend towards increasing carbon losses in the Northern Hemisphere (north of 25°N) at a rate of 13 Tg C yr^{-1} ($P = 0.01$) during 1980–2002. In the ORCHIDEE model long-term simulation, the increasing autumn source of carbon to the atmosphere offsets about 90% of the increasing carbon sink in spring. This result is consistent with the atmospheric concentration analysis (Supplementary Table 3). We attribute the trend in net carbon loss during autumn to increases in TER (21 Tg C yr^{-1}) dominating over increasing GPP (8 Tg C yr^{-1}) owing to delayed leaf senescence. In autumn, both modelled GPP and TER increase with increasing temperature, but the temperature sensitivity of TER ($5.0 \text{ g C m}^{-2} \text{ }^\circ\text{C}^{-1}$) exceeds that of GPP ($2.5 \text{ g C m}^{-2} \text{ }^\circ\text{C}^{-1}$). This is due to limitations of radiation and temperature on GPP during the autumn²⁴, and to soil desiccation carried over from the summer dry period²¹. As a result, autumn NEP is simulated to be an increasing source of CO₂ in response to warming, with a mean sensitivity of $-2.5 \text{ g C m}^{-2} \text{ }^\circ\text{C}^{-1}$ (or about $-0.2 \text{ Pg C }^\circ\text{C}^{-1}$ north of 25°N), which is comparable to that derived from eddy-covariance measurements ($-3.2 \text{ g C m}^{-2} \text{ }^\circ\text{C}^{-1}$; Fig. 2).

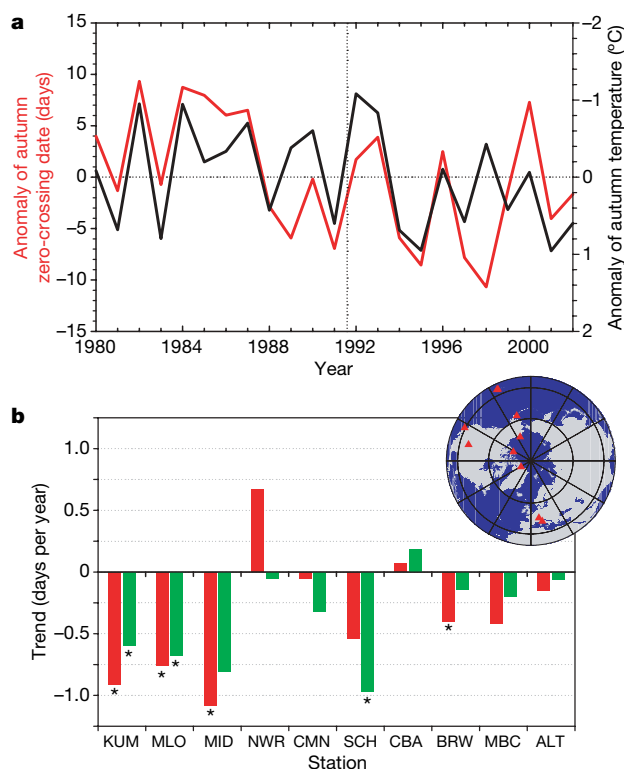


Figure 1 | Atmospheric CO₂ concentration data analysis from long-term records of the global NOAA-ERSL air-sampling network. **a**, Interannual variability in anomaly of upward zero-crossing date (red) observed at Point Barrow, Alaska, and the corresponding autumn (September to November) temperature (black) over the region between 51° and 90°N over the past two decades. Upward zero-crossing date is strongly anti-correlated with autumn temperature (slope = $-5.4 \text{ days }^\circ\text{C}^{-1}$; $R = -0.61$, $P = 0.002$). The vertical dotted line indicates the time of the eruption of Mount Pinatubo. **b**, Trends in upward zero-crossing date (red) and length of the net CUP (green) from long-term Northern Hemisphere atmospheric observations during at least the past 15 years (see Methods). The differences in the trends between autumn upward zero-crossing date and CUP reflects changes in the spring downward zero crossing. As a result of the earlier autumn upward zero-crossing date, CUP has persistently decreased by an average of 0.36 ± 0.38 days per year since 1980. The inset shows the distribution of the stations used in this study. Station abbreviations are defined in Supplementary Table 1.

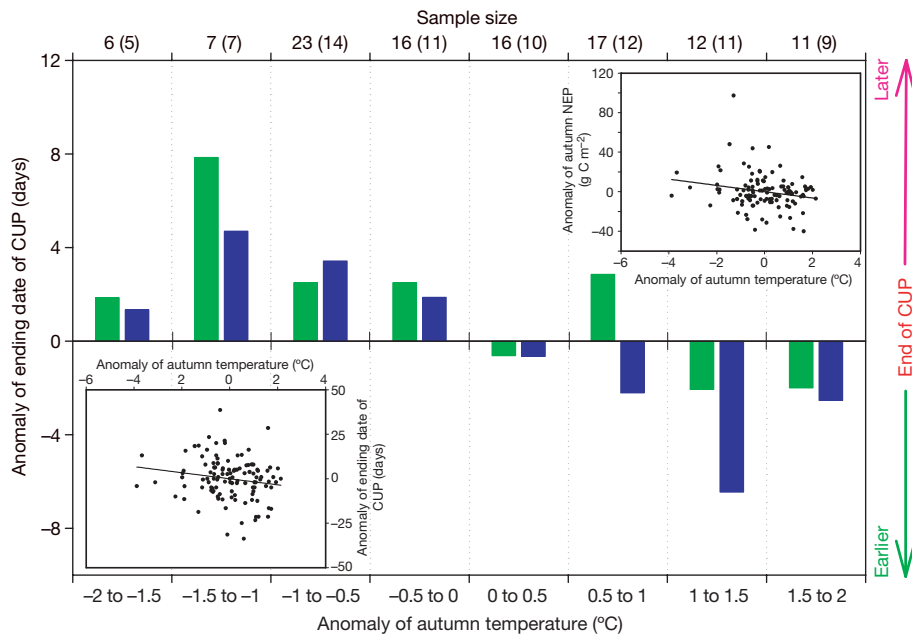


Figure 2 | Eddy-covariance flux data analysis from boreal sites in North America and Eurasia. A total of 108 site-years have been aggregated in this figure. The average (blue) and median (green) anomaly of ending date of net CUP is shown for different autumn temperature anomalies binned into $0.5\text{ }^{\circ}\text{C}$ intervals. The top horizontal axis labels correspond to the number of site-years and sites (in parenthesis) in each temperature bin. The bottom left inset shows the relationships between ending date of CUP and temperature anomalies. There is a marginally negative correlation between autumn CUP ending date and temperature anomalies ($y = -1.7x - 0.0087$, $P = 0.07$). If we exclude the four site-years with the most extreme cold anomalies ($\Delta T < -2\text{ }^{\circ}\text{C}$), the negative correlation between CUP ending date and temperature becomes highly significant ($P = 0.03$) and the slope is steeper ($y = -2.4x + 0.3007$), suggesting that below a certain threshold of cold anomaly there is no further decrease in respiration. The top right inset shows the relationships between autumn NEP and temperature anomalies. A positive NEP value indicates an increased carbon uptake. Autumn was defined as the 60-day interval around the average CUP ending date for each site. Eddy-covariance data show increased carbon losses under warmer conditions, with a temperature sensitivity of NEP of $-3.2\text{ g C m}^{-2}\text{ }^{\circ}\text{C}^{-1}$ ($y = -3.17x - 5 \times 10^{-6}$, $P = 0.04$).

Our results suggest that net carbon uptake of northern ecosystems is being decreased in response to autumnal warming. The spatial distribution of the response of carbon flux to temperature, as projected by the ORCHIDEE model, is shown in Fig. 3. Warmer autumns coincide with greater than normal GPP (Fig. 3a). However, because of a concurrent stimulation of plant respiration, the geographical area where autumn NPP increases with temperature (slope $> 5\text{ g C m}^{-2}\text{ }^{\circ}\text{C}^{-1}$) is much less extensive than the area where GPP increases (Fig. 3b). The spatial pattern of the autumn increase in NPP in response to warming is remarkably similar to that of the NOAA/AVHRR vegetation index (NDVI) data²⁵ (Fig. 3d), suggesting that results from the ORCHIDEE model for NPP are realistic. However, this 'extra' autumn NPP is being accompanied by even more respiration in response to warming, so that the modelled NEP response shows systematic anomalous carbon losses during warmer autumns, in particular over North America and Europe (Fig. 3c).

Observed historical climate data⁵ reveal that Eurasia experienced a stronger warming in spring ($0.06\text{ }^{\circ}\text{C yr}^{-1}$, $P = 0.001$) than in autumn ($0.02\text{ }^{\circ}\text{C yr}^{-1}$, $P = 0.15$) over the past two decades. In contrast, North America has experienced a larger warming in autumn ($0.05\text{ }^{\circ}\text{C yr}^{-1}$, $P = 0.03$) than in spring ($0.02\text{ }^{\circ}\text{C yr}^{-1}$, $P = 0.36$). In addition, a more significant and coherent greening pattern in Eurasia than in North America has been detected in the remote sensing data⁷. This suggests that the processes and the magnitude of seasonal changes in NEP in Eurasia and North America are different, which may control the annual carbon balance of their ecosystems. Further constraints on the spatial and temporal patterns of large-scale ecosystem fluxes will be delivered in the future from atmospheric inversions constrained with longer-term ecosystem flux data.

Applying the future Northern Hemisphere warming of $3.8\text{--}6.6\text{ }^{\circ}\text{C}$ predicted by a climate model²⁶ to the sensitivity of the autumn zero-crossing date of atmospheric CO_2 at Point Barrow (about $5\text{ days }^{\circ}\text{C}^{-1}$) gives a projected advance of $19\text{--}33\text{ days}$ by the end of the twenty-first century. Previous model assessments of the response of land ecosystems to climate change concluded that terrestrial carbon sinks should peak by about the year 2050 and then diminish towards the end of the twenty-first century^{9,10}. The asymmetrical

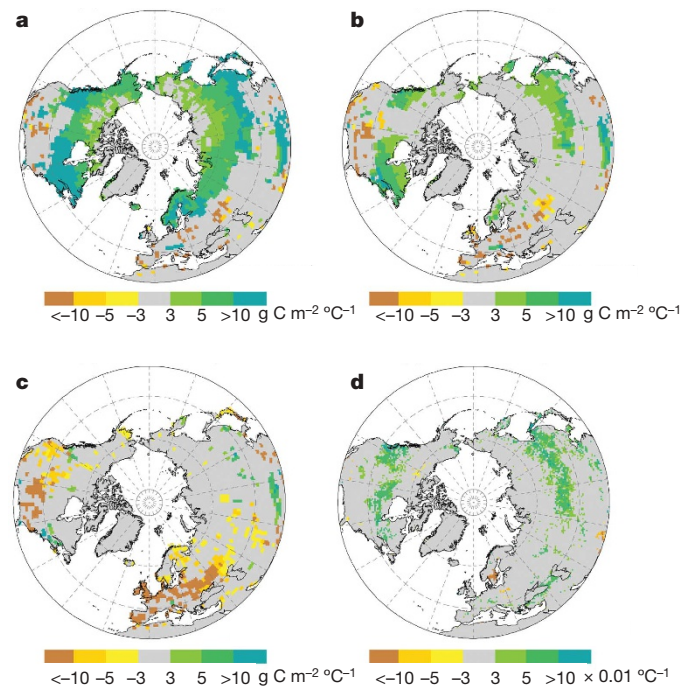


Figure 3 | A model view of the spatial distribution of the effects of autumn (September to November) temperature warming on gross and net carbon fluxes, obtained with the ORCHIDEE model. a, ORCHIDEE model-derived autumn GPP. b, ORCHIDEE model-derived autumn NPP. c, ORCHIDEE model-derived autumn NEP. d, Sum of satellite-derived autumn normalized difference vegetation index (NDVI). The sensitivity is expressed as the linearly regressed slope of autumn carbon flux or of NDVI against autumn temperature for each pixel over the past two decades. A positive slope of NEP indicates that terrestrial carbon uptake is increasing with warmer temperatures, and vice versa. Areas with a low sensitivity or insignificant ($P > 0.05$) relationships between the variables are coloured in grey.

impact of autumn versus spring warming on ecosystem carbon exchange contributes significant uncertainty to future projections. If warming in autumn occurs at a faster rate than in spring, the ability of northern ecosystems to sequester carbon may diminish in the future. Acquiring a greater understanding of responses of terrestrial ecosystems to climate trends at the edges of the growing season, including potential acclimation processes, is clearly a priority, and should come from controlled ecosystem experiments and long-term eddy-covariance data sets.

METHODS SUMMARY

We analysed the effects of autumn temperature on the carbon balance of northern ecosystems at different scales, using three different methods.

First, we used smoothed flask CO₂ data from the NOAA/ESRL network²⁰ to characterize changes in the seasonal CO₂ zero-crossing dates^{18,27} for ten stations over the Northern Hemisphere (Fig. 1). We correlated each zero-crossing date with the corresponding observed temperature⁵ or precipitation⁵ in spring (March to May) and autumn (September to November), and with the ORCHIDEE¹⁶-modelled soil moisture content. The trends in CO₂ zero-crossing dates and their correlation with climate factors were computed by using linear least-squares regression. The significance of statistical analyses in this study were assessed on the basis of two-tailed significance tests. To isolate further the contribution of fluxes and transport to the year-to-year atmospheric CO₂ signal, we performed factorial simulation experiments in which NEP from the ORCHIDEE¹⁶ vegetation model forced by varying climate fields⁵ provided surface boundary conditions for simulated CO₂ in the atmospheric transport model LMDZt¹⁷ driven by interannual winds.

Second, we analysed the net CO₂ flux data measured by the eddy-covariance technique from 24 northern ecosystem sites (Supplementary Table 4). The end of the CUP is defined as the last day in a year when the NEP five-day running means exceed zero. Autumn is defined as the interval of ± 30 days around the average CUP ending date at each site. We grouped the 108 year-site data into distinct 0.5 °C bins of autumn temperature anomaly. For each autumn temperature bin we calculated the median and mean anomaly of the ending date of the CUP.

Third, hints on the processes that control the integrated autumn NEP response to temperature, through the individual sensitivity of photosynthesis and respiration, were provided by integrating the ORCHIDEE vegetation model¹⁶ forced by historic climate data⁵ during the period 1980–2002.

Full Methods and any associated references are available in the online version of the paper at www.nature.com/nature.

Received 16 April; accepted 6 November 2007.

- Goulden, M. L. *et al.* Sensitivity of boreal forest carbon balance to soil thaw. *Science* **279**, 214–217 (1998).
- Randerson, J. T., Field, C. B., Fung, I. Y. & Tans, P. P. Increases in early season ecosystem uptake explain recent changes in the seasonal cycle of atmospheric CO₂ at high northern latitudes. *Geophys. Res. Lett.* **26**, 2765–2768 (1999).
- Morgenstern, K. *et al.* Sensitivity and uncertainty of the carbon balance of a Pacific Northwest Douglas-fir forest during an El Niño La Niña cycle. *Agric. For. Meteorol.* **123**, 201–219 (2004).
- Bergeron, O. *et al.* Comparison of carbon dioxide fluxes over three boreal black spruce forests in Canada. *Glob. Change Biol.* **13**, 89–107 (2007).
- Mitchell, T. D. & Jones, P. D. An improved method of constructing a database of monthly climate observations and associated high-resolution grids. *Int. J. Climatol.* **25**, 693–712 (2005).
- Myneni, R. B., Keeling, C. D., Tucker, C. J., Asrar, G. & Nemani, R. R. Increased plant growth in the northern high latitudes from 1981 to 1991. *Nature* **386**, 698–702 (1997).
- Zhou, L. M. *et al.* Variations in northern vegetation activity inferred from satellite data of vegetation index during 1981 to 1999. *J. Geophys. Res.* **106**, 20069–20083 (2001).
- Churkina, G., Schimel, D., Braswell, B. H. & Xiao, X. M. Spatial analysis of growing season length control over net ecosystem exchange. *Glob. Change Biol.* **11**, 1777–1787 (2005).
- Cramer, W. *et al.* Global response of terrestrial ecosystem structure and function to CO₂ and climate change: results from six dynamic global vegetation models. *Glob. Change Biol.* **7**, 357–373 (2001).

- Sitch, S. *et al.* Evaluation of the terrestrial carbon cycle, future plant geography and climate–carbon cycle feedbacks using 5 Dynamic Global Vegetation Models (DGVMS). *Glob. Change Biol.* (in the press).
- Black, T. A. *et al.* Increased carbon sequestration by a boreal deciduous forest in years with a warm spring. *Geophys. Res. Lett.* **27**, 1271–1274 (2000).
- Tanja, S. *et al.* Air temperature triggers the recovery of evergreen boreal forest photosynthesis in spring. *Glob. Change Biol.* **9**, 1410–1426 (2003).
- Menzel, A. *et al.* European phenological response to climate change matches the warming pattern. *Glob. Change Biol.* **12**, 1969–1976 (2006).
- Schwartz, M. D., Ahas, R. & Aasa, A. Onset of spring starting earlier across the Northern Hemisphere. *Glob. Change Biol.* **12**, 343–351 (2006).
- IPCC. *Climate Change 2007: The Physical Sciences Basis: Contribution of Working Group I to the Fourth Assessment Report of the Intergovernmental Panel on Climate Change* (Cambridge Univ. Press, Cambridge, 2007).
- Krinner, G. *et al.* A dynamic global vegetation model for studies of the coupled atmosphere–biosphere system. *Glob. Biogeochem. Cycles* **19**, doi:10.1029/2003GB002199 (2005).
- Hourdin, F. & Armengaud, A. The use of finite-volume methods for atmospheric advection of trace species. Part I: Test of various formulations in a general circulation model. *Mon. Weath. Rev.* **127**, 822–837 (1999).
- Keeling, C. D., Chin, J. F. S. & Whorf, T. P. Increased activity of northern vegetation inferred from atmospheric CO₂ measurements. *Nature* **382**, 146–149 (1996).
- Heimann, M. *et al.* Evaluation of terrestrial carbon cycle models through simulations of the seasonal cycle of atmospheric CO₂: First results of a model intercomparison study. *Glob. Biogeochem. Cycles* **12**, 1–24 (1998).
- GLOBALVIEW-CO₂. *Cooperative Atmospheric Data Integration Project Carbon Dioxide*, (<ftp.cmdl.noaa.gov/ccg/co2/GLOBALVIEW>) (2004).
- Angert, A. *et al.* Drier summers cancel out the CO₂ uptake enhancement induced by warmer springs. *Proc. Natl Acad. Sci. USA* **102**, 10823–10827 (2005).
- Linderholm, H. W. Growing season changes in the last century. *Agric. For. Meteorol.* **137**, 1–14 (2006).
- Ciais, P. *et al.* Europe-wide reduction in primary productivity caused by the heat and drought in 2003. *Nature* **437**, 529–533 (2005).
- Piao, S. L., Friedlingstein, P., Ciais, P., Zhou, L. M. & Chen, A. P. Effect of climate and CO₂ changes on the greening of the Northern Hemisphere over the past two decades. *Geophys. Res. Lett.* **33**, doi:10.1029/2006GL028205 (2006).
- Myneni, R. B. & Song, X. *NDVI Version 3 based on Pathfinder*, (ftp://primavera.bu.edu/pub/datasets/AVHRR_DATASETS/PATHFINDER/VERSION3_DATA/) (2003).
- Marti, O. *et al.* *The New IPSL Climate System Model: IPSL-CM4* (Institut Pierre Simon Laplace, Paris, 2006).
- Thoning, K. W., Tans, P. P. & Komhyr, W. D. Atmospheric carbon-dioxide at Mauna Loa Observatory. 2. Analysis of the NOAA GMCC data, 1974–1985. *J. Geophys. Res.* **94**, 8549–8565 (1989).

Supplementary Information is linked to the online version of the paper at www.nature.com/nature.

Acknowledgements We thank all the people and their respective funding agencies who worked to provide data for this study, and specifically B. Amiro, M. A. Arain, T. A. Black, C. Bourque, L. Flanagan, J. H. McCaughey and S. Wofsy for providing some of the flux data from the Canadian sites, and M.-A. Giasson and C. Coursolle for their help in compiling the data. We also thank A. Friend, P. Rayner and N. Viovy for helpful comments and discussions. This study was supported by European Community-funded projects ENSEMBLES and CARBOEUROPE IP, and by the National Natural Science Foundation of China as well as by Fluxnet-Canada, which was supported by CFCAS, NSERC, BIOCAP, MSC and NRCan. The computer time was provided by CEA. We thank the NOAA-ERSL global air sampling program for collecting and analysing the long-term CO₂ flask data, and K. Masarie at NOAA-ERSL for generating each year the GLOBALVIEW-CO₂ collaborative data product, which formed the basis of our atmospheric data analysis. The ongoing exchange of ideas, data and model results in the international research community on the carbon cycle is facilitated by the Global Carbon Project.

Author Contributions P.C., S.P., P.F. and P.P. designed the research. S.P., P.C. and P.F. performed ORCHIDEE modelling analysis. P.P. and S.P. performed transport analysis. S.P., S.L., M.R., H.M. and P.C. performed eddy-covariance data analysis. S.P., P.C. and J.F. performed satellite data analysis. All authors contributed to the interpretation and writing.

Author Information Reprints and permissions information is available at www.nature.com/reprints. Correspondence and requests for materials should be addressed to S.L.P. (slpiao@lsce.ipsl.fr) or P.C. (philippe.ciais@lsce.ipsl.fr).

METHODS

Atmospheric CO₂ data. We used flask data from the NOAA/ESRL network to characterize trends in the CO₂ zero-crossing dates (spring downward and autumn CO₂ upward) that correspond roughly to the time of maximum NEP uptake in spring and maximum release in autumn. Following the approach described in ref. 27, we first removed the interannual trend in the atmospheric CO₂ concentration for each site with a polynomial curve of degree 2, four harmonic seasonal function, and time-filtered residuals. We then used the harmonics plus the residuals (detrended CO₂ seasonal cycle) to define the downward and upward CO₂ zero-crossing dates as the day on which the detrended curve crossed the zero line from positive to negative and from negative to positive, respectively. We considered only northern stations for which at least 15 years of data were available during the period 1980–2002 (Supplementary Table 1).

The downward and upward CO₂ zero-crossing dates were correlated with spring (March to May) and autumn (September to November) air temperature⁵ over a broad region surrounding each station by $\pm 20^\circ$ of latitude, respectively (Supplementary Table 1). Using a similar method, we also evaluated the correlation with precipitation⁵ and modelled change in soil moisture¹⁶.

Eddy-covariance data. The eddy-covariance CO₂ flux observations were performed in accordance with the routine procedures established by regional networks (for example, Fluxnet-Canada and CARBOEUROPE²⁸). Half-hourly data were quality-controlled, filtered against low turbulence by using friction velocity as a heuristic criterion and gap-filled by the method developed in ref. 29. Data were aggregated to daily flux integrals and were only used for the analyses if more than 80% of the half-hourly values were either direct measurements or gap-filled with high confidence. The end of the CUP was calculated as the last day in a year when NEP five-day running means exceeded zero; that is, when the ecosystems became a source of CO₂ to the atmosphere. Autumn was defined as the period during ± 30 days of the average ending date of CUP for each site. Because the flux records are not long enough to assess the long-term impact of autumn temperature trends on the ending date of CUP and net CO₂ exchange for each site, we grouped the 108 year-site data into different 0.5 °C bins of autumn temperature anomaly. For each bin we calculated the median and average anomaly of the ending date of CUP. To ensure the reliability of the statistical analysis of median and average calculation, we used only the data in temperature classes with a sample size greater than 3.

Global vegetation model. The global vegetation model called ORCHIDEE ('ORganizing Carbon and Hydrology In Dynamic Ecosystems')¹⁶ was used to simulate the terrestrial biogeochemical processes. ORCHIDEE describes the turbulent surface fluxes of CO₂, water and energy (transpiration, photosynthesis and respiration), the dynamics of water and carbon pools (soil moisture budget and allocation, growth, mortality, and soil carbon decomposition) and longer-term ecosystem dynamics (fire, sapling establishment and light competition). Fluxes were calculated each hour, and carbon pools were updated each day. Onset and senescence of foliage development depend on a critical leaf age, water and temperature stresses¹⁶.

With the use of 1901 climate data and the 1860 atmospheric CO₂ concentration of 286 p.p.m., a first model spin-up was performed to bring carbon pools to equilibrium. A second spin-up was performed with interannually variable climate data over 1901–1910 to define the initial condition of a run covering 1901–2002. The monthly climate data sets were supplied by the Climatic Research Unit, University of East Anglia, UK³. These data were transformed to half-hourly weather variables by using a weather generator³⁰.

The modelled NEP over 1980–2002, prescribed in an atmospheric transport model (LMDzt), was found to faithfully reproduce the interannual variations in the spring drawdown date and autumn build-up date at high-latitude (north of 50° N) stations that are predominantly affected by the fluxes of the Northern Hemisphere (Supplementary Table 3 and Supplementary Fig. 1). Furthermore, the modelled upward zero crossing at high-latitude (north of 50° N) stations has advanced by an average of -0.19 ± 0.05 days yr⁻¹, which is comparable to that estimated from atmospheric CO₂ concentration data (-0.22 ± 0.23 days yr⁻¹).

Atmospheric transport model. We used the three-dimensional eulerian transport model LMDzT derived from the general circulation model of the Laboratoire de Météorologie Dynamique, LMDz¹⁷, to compute the daily CO₂ concentration at each station driven by daily NEP variations from ORCHIDEE during 1980–2002. The model has a horizontal resolution of $3.75^\circ \times 2.5^\circ$ and 19 vertical levels. The simulated winds are relaxed towards the analysed field of ECMWF ('nudging' mode) and therefore vary from year to year according to the observations. Advection, deep convection and turbulent mixing of tracer are calculated by following the schemes proposed in refs 31, 32 and 17, respectively.

To separate the effects of transport and terrestrial carbon fluxes on the zero-crossing date signal, we performed two simulations. The first one used interannual daily NEP fluxes calculated during the period 1980–2002 by ORCHIDEE. The second simulation (referred to as 'transport only') used climatological but daily variable NEP. The contribution of interannually varying fluxes to the variability in zero-crossing date is assessed by the difference in simulated atmospheric CO₂ between the first and the second simulations, which is referred to as 'flux only'. In addition, we computed the contribution to CO₂ concentrations from air–sea exchange and fossil fuel emissions and their increase (annual increase per group of countries) by following estimates from refs 33 and 34, respectively. Because of the lack of information on seasonal variations of fossil fuel emissions, we tested the impact of possible changes in fossil seasonality using the method of ref. 35 to construct seasonally varying fossil fuel emission. We modelled the impact on atmospheric CO₂ in the LMDzT transport model of using a modified fossil fuel source with seasonal amplitude of 40%, 20%, 10%, 5% and 0%. The results showed that the change in zero-crossing date is less than 1.3 days, even when the seasonal amplitude of fossil fuel emissions changed by 40%.

28. Aubinet, M. *et al.* Estimates of the annual net carbon and water exchange of forest: the EUROFLUX methodology. *Adv. Ecol. Res.* **30**, 113–175 (2000).
29. Papale, D. *et al.* Towards a standardized processing of Net Ecosystem Exchange measured with eddy covariance technique: algorithms and uncertainty estimation. *Biogeosciences* **3**, 571–583 (2006).
30. Richardson, C. W. & Wright, D. A. *A Model for Generating Daily Weather Variables*, Technical Report (US Department of Agriculture, Agricultural Research Service, Washington DC, 1984).
31. van Leer, B. Towards the ultimate conservative difference scheme: IV. A new approach to numerical convection. *J. Comput. Phys.* **23**, 276–299 (1977).
32. Tiedtke, M. A comprehensive mass flux scheme for cumulus parameterization in large-scale models. *Mon. Weath. Rev.* **117**, 1779–1800 (1989).
33. Takahashi, T. *et al.* in *Extended Abstracts of the 2nd International CO in the Oceans Symposium* 18–01 (Tsukuba, Japan, 1999).
34. Marland, G., Boden, T. A. & Andres, R. J. *Global, Regional, and National CO₂ Emissions. Trends: A Compendium of Data on Global Change*. (http://cdiac.esd.ornl.gov/trends/emis/tre_glob.htm) (2007).
35. Gurney, K. R. *et al.* Sensitivity of atmospheric CO₂ inversions to seasonal and interannual variations in fossil fuel emissions. *J. Geophys. Res.* **110**, doi:10.1029/2004JD005373 (2005).